Summer 2010

Modeling Particle Transport Distances as a Function of Slope and Surface Roughness

Morgan K. Mendoza
San Jose State University

MODELING PARTICLE TRANSPORT DISTANCES AS A FUNCTION OF SLOPE AND SURFACE ROUGHNESS

A Thesis

Presented to

The Faculty of the Department of Geology

San José State University

In Partial Fulfillment

of the Requirements for the Degree

Master of Science

by

Morgan Kelly Mendoza

August 2010

The Designated Thesis Committee Approves the Thesis Titled

MODELING PARTICLE TRANSPORT DISTANCES AS A FUNCTION OF SLOPE AND SURFACE ROUGHNESS

by

Morgan Kelly Mendoza

APPROVED FOR THE DEPARTMENT OF GEOLOGY

SAN JOSÉ STATE UNIVERSITY

August 2010

Dr. Emmanuel Gabet	Department of Geology
Dr. Paula Messina	Department of Geology
Dr. Richard Sedlock	Department of Geology

ABSTRACT

MODELING PARTICLE TRANSPORT DISTANCES AS A FUNCTION OF SLOPE AND SURFACE ROUGHNESS

by Morgan Kelly Mendoza

Significant effort has been put into modeling the evolution of hillslope profiles through time. The models use a continuum approach and are commonly deterministic. Early models assumed a linear relationship between hillslope angle and sediment flux. This relationship produces hillslope profiles that increase in steepness from crest to base. However, hillslopes observed in the field are commonly planar downslope of their convex crests. Recently, non-linear sediment transport equations have been developed that produce hillslope profiles closer to those which are observed in nature, yet the mid-slope sections are not entirely planar. Currently, there is interest in using a non-deterministic approach where transport distances follow probability distributions that depend on hillslope angle. In order to qualitatively and quantitatively characterize this probabilistic relationship, the transport distances of individual particles released into a dry ravel flume with a rough surface were measured as a function of flume angle. Using the inputs of flume angle and surface roughness, the results of the experiments were replicated with a discrete element model in which the motion of the particles was modeled with the momentum equation. The implication of this study is that this method can be used with inputs measured from the field to model the evolution of entire hillslopes.

TABLE OF CONTENTS

LIST OF FIGURES

Figure

LIST OF TABLES

Table

INTRODUCTION

Culling (1960) hypothesized that the mass movement of weathered material on a hillslope takes place at a rate proportional to the surface gradient. Culling (1963) was subsequently able to show that when soil particles are assumed to move according to a random walk process, the overall behavior of soil on a hillslope follows a linear diffusion-like equation. By coupling this linear diffusion equation with the continuity equations, hillslope profiles at steady-state can be determined. This approach avoids the need to consider each particle of soil individually and, instead, assumes that soil is a continuum.

The type of linear continuum model proposed by Culling (1963) predicts hillslopes with constant curvature; however, hillslopes found in nature are commonly convex near their crests with planar mid-slope sections. To reconcile this field observation with linear models, some (Kirkby, 1985; Anderson, 1994) have suggested that the angle associated with the planar mid-slope section represents the transition to landslide-dominated hillslopes. Others have appealed to a non-linear approach (e.g., Roering et al., 1999; Gabet, 2000) in which sediment flux increases rapidly at steep slopes toward a critical gradient at which the sediment flux becomes infinite. Sharp increases in the sediment flux at higher slopes may be the result of greater amounts of sediment transported, greater average transport distances, or both. The latter has been observed in sediment transported by gopher bioturbation (Gabet, 2000), dry ravel (Gabet, 2003), and raindrop impact (Furbish et al., 2009). Roering et al. (2001) developed a non-linear equation for sediment flux and used it as the basis for a hillslope evolution model. The model produces hillslope profiles that agree with field observations, though it is not able to produce perfectly planar hillslopes.

Continuum models, such as the ones introduced by Culling (1960, 1963), depend on two main assumptions: (1) the average sediment mass flow rate can be approximated using hillslope gradient without the need to account for the exact movement of each individual particle, and (2) the gradient need be known only at a single point in order to generate an accurate prediction of the mass flow at that point (Tucker and Bradley, 2010). These are locality assumptions, which are not unique to hillslope transport, and are used whenever it is assumed that particles on a hillslope move only short distances relative to the length of the hillslope (Schumer et al., 2009). In contrast, nonlocal sediment transport occurs when the distance that a particle travels is large relative to the length of the hillslope. Specifically, nonlocality occurs when the mean distance traveled by a particle tends toward infinity and, as a result, the probability distribution associated with the transport distance develops a heavy tail that is right-skewed (Tucker and Bradley, 2010). If nonlocal behavior is observed, then the concentration and momentum of particles at a point cannot be accurately estimated based solely on the hillslope gradient at that point (Tucker and Bradley, 2010).

Recently, there has been a shift away from approaches that are deterministic and that assume particles on a hillslope form a continuum, in favor of gaining a more detailed understanding of hillslope sediment transport processes (e.g., Tucker and Bradley, 2010). If the position and momentum of each particle on a hillslope were known, along with the rules that governed the interactions between grains, the magnitude and direction of the volumetric sediment flux could be calculated at any given point. This technique is known as the discrete element approach; however, because it is computationally prohibitive to model the grain-to-grain interactions of every particle on an entire hillslope, the motion of the particles can instead be modeled in a statistical fashion (Tucker and Bradley, 2010).

To characterize the individual motion of sand grains, Roering (2004) performed a series of experiments in which sand was piled into an open-ended box with Plexiglass sides and then perturbed by acoustic vibrations. By placing clumps of colored tracer grains into the pile at various depths, Roering (2004) was able to measure the displacement of the grains after they had been perturbed. The distance traveled by buried particles could be modeled deterministically because the grains remained clumped, whereas grains that had been buried less than 1 cm dispersed and traveled large and variable distances, suggesting that the travel distance of particles near the surface is better characterized probabilistically (Roering, 2004).

Recognizing that transport distances are not deterministic, Furbish and Haff (2010) used a probabilistic approach to model continuity of mass at a point, given random arrivals and departures to and from the point. This model was incorporated into a master equation that describes geomorphic systems. Furbish and Haff (2010) assumed an exponential distribution for transport distances of particles, and the model results are in agreement with field observations, but are not able to produce perfectly planar hillslopes. Some of the key parametric quantities in the model of Furbish and Haff (2010) are well constrained for certain transport processes but not for others. For example, in the case of rain splash, the use of an exponential distribution for transport distances is justified (Furbish et al., 2007), but other processes may give rise to different distributions. Furbish and Haff (2010) conjectured that hillslope gradient would be a main factor in the formulation of such distributions but that surface roughness and sediment characteristics would likely be involved.

Sediment transport laws can be developed that are based not on random walks, but on the type of motion that is actually observed for individual particles (Tucker and Bradley, 2010). In order to develop such sediment transport laws,

experiments would need to be performed that measure the frequency with which particles travel certain distances, and their mean and variance. In addition, it would need to be established that the results of such experiments could be tied to the physical characteristics of a hillslope (e.g., gradient and roughness). Tucker and Bradley (2010) developed a computer model in which one particle out of a large mound of individual particles is randomly selected to make a "hop." However, whether the particle will actually make a hop is dependent on its position relative to its neighbors and on a probability distribution. This model has the advantage of being discrete, nondeterministic, and computationally efficient; however, the probability distribution was chosen arbitrarily and was not based on experimental results.

Although there has been interest in gaining a more detailed understanding of hillslope sediment transport processes with an increasing emphasis on discrete and probabilistic approaches, data on transport distances of actual particles are limited. This study examines the simplest hillslope transport process, dry ravel, defined as the rolling, sliding, and bouncing of particles down a rough surface. The purpose of this study is twofold: (1) to develop an approach to model transport distances of particles that depends on roughness and slope, preserves the essential physics of the process, and is parsimonious; and (2) to mathematically describe the probability distribution of transport distances as a function of flume angle.

MATERIALS AND METHODS

The main piece of equipment used was a 3-m-long, 0.3-m-wide, 0.1-m-deep wooden box. The floor of the box consisted of a layer of concrete into which pebbles with diameters ranging from 1-5 cm had been embedded to simulate the rough

surface of a hillslope. This box is hereafter referred to as "the dry ravel flume" (Fig. 1).

To characterize the roughness of the flume surface, its elevation was measured along width-parallel transects at 1 cm intervals. The surface relief along each transect was calculated by subtracting the mode of the transect elevations from each measurement and then taking the absolute value of the result. Transects were taken along the entire length of the flume at 10 cm intervals, for a total of 28 width parallel transects. Twenty-nine measurements were taken for each transect, for a total of 812 calculated values of the surface relief, to form a distribution that characterizes the roughness of the flume surface.

A hopper was used to impart an initial velocity to the 1-cm pebbles used in the flume experiments. The hopper quickly released a pebble from rest at a controlled height onto a short (5 cm) wooden ramp inclined at 11° (Fig. 2). This method was adopted to ensure that the initial velocity of the pebbles in the down-flume direction was as uniform as possible (Gabet, 2003). The velocity initially directed down-flume is proportional to the sine of the flume angle. Because sine is an increasing function of flume angle, the release height of the pebbles was decreased with increasing flume angle, such that the initial velocity, v_o, remained constant (0.7 m/s) throughout the experiments. Release height, h, was adjusted according to:

$$v_o = \sqrt{2gh} sin(\theta + 11), \tag{1}$$

where g is acceleration due to gravity, and θ is flume angle.

The experiments consisted of releasing a pebble into the flume, measuring its travel distance, and then removing it. This was repeated 100 times at each angle setting. The angle of the flume was varied in increments of 3°, starting from 0°. As

Figure 1. Dry ravel flume used in experiments.

Figure 2. Hopper, ramp, and pebbles shown on dry ravel flume.

the experiments progressed to steeper flume angles, some of the pebbles did not stop and instead rolled to the end of the flume. If this occurred, the distance traveled was recorded as "infinity." Eventually the flume reached an angle, 30°, where all 100 pebbles rolled to the end. At this point the experiment was terminated.

RESULTS

The average distance traveled by the pebbles increased nonlinearly with angle (Fig. 3). At 3° there is an anomalous dip in the average transport distance; however, given the variance of the data it is not significantly less than the average transport distance at 0° (p-value=0.149, see Appendix II for details). The proportion of pebbles that rolled to the end of the flume increased as the flume angle increased (Fig. 4). The distributions of transport distances are skewed, and as the slope steepens, the peak occurs at higher values and the range increases (Fig. 5). For the flume angles where a significant proportion of pebbles rolled to the end (18°- 24°) the distributions flatten out and become quasi-uniform. At 27°, only four pebbles stopped on the ramp, making it difficult to draw conclusions about the shape of the distribution.

To mathematically describe the probability distribution of the transport distances as a function of flume angle, let X be a random variable which takes on the values 1 and 0, associated with success and failure respectively. The event in which a particle stops on the flume is defined to be a success and the event in which a particle rolls to the end of the flume is defined to be a failure. $X \sim \text{Bernoulli}(p)$, with probability mass function:

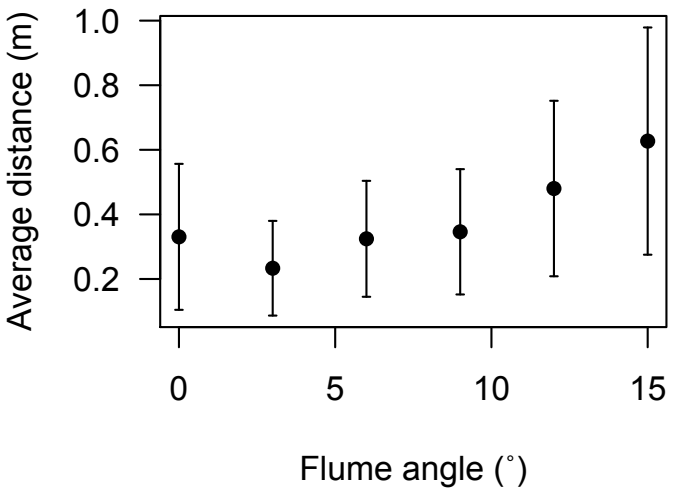

Figure 3. Average transport distance ($\pm 1\sigma$) as a function of slope obtained from flume experiments. Beyond 15°, some pebbles reached the end of the flume and therefore an average distance could not be calculated.

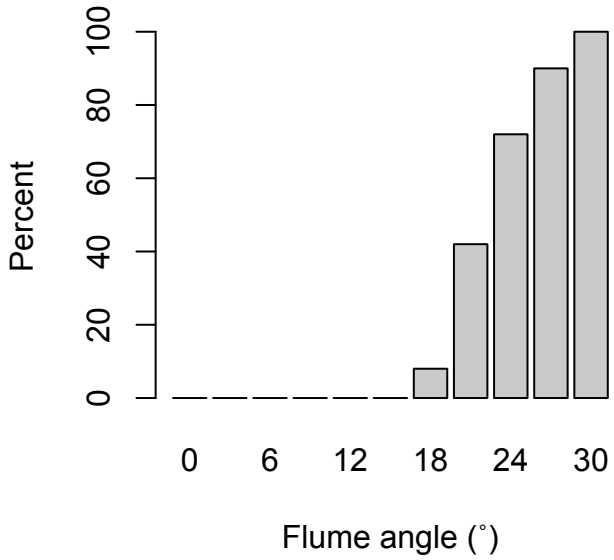

Figure 4. Proportion of pebbles that rolled to end of flume during experiments as a function of flume angle.

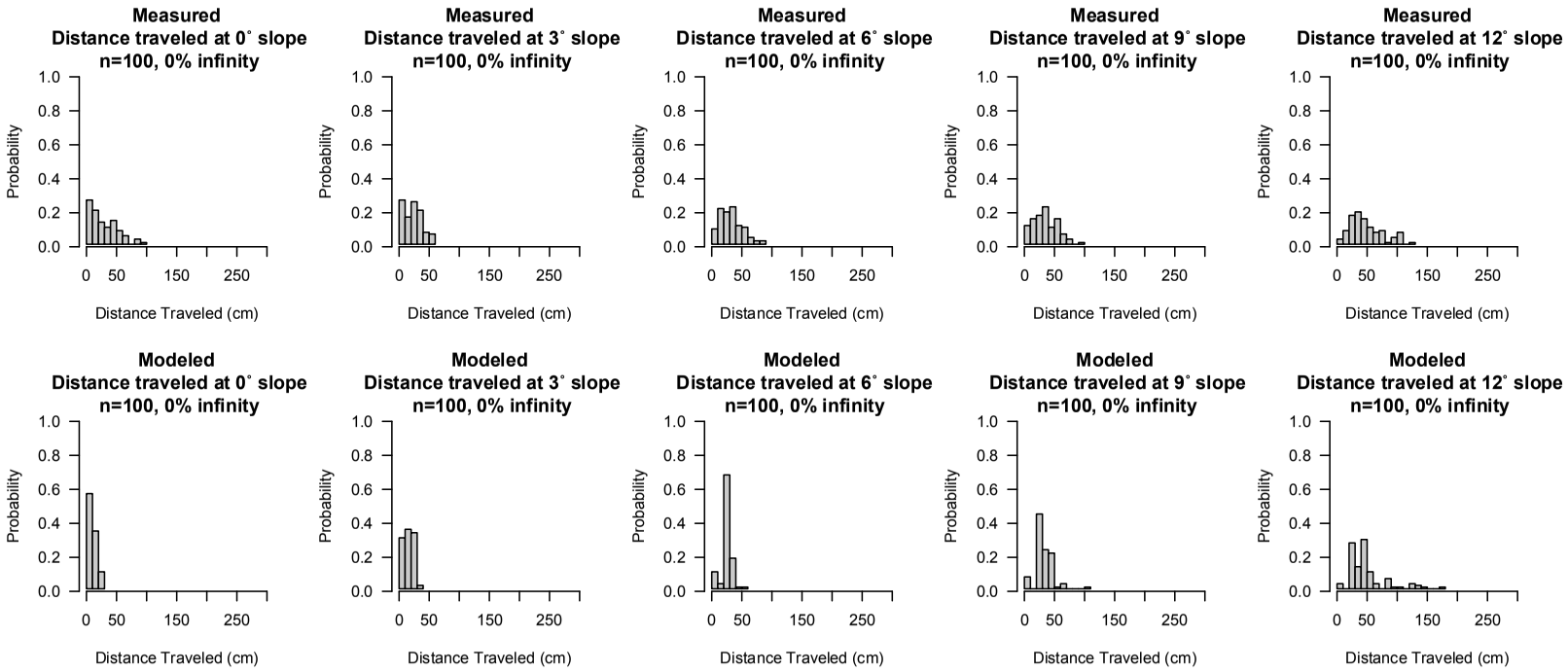

Figure 5. Comparison of distributions of measured and modeled distances traveled. Continued on next page.

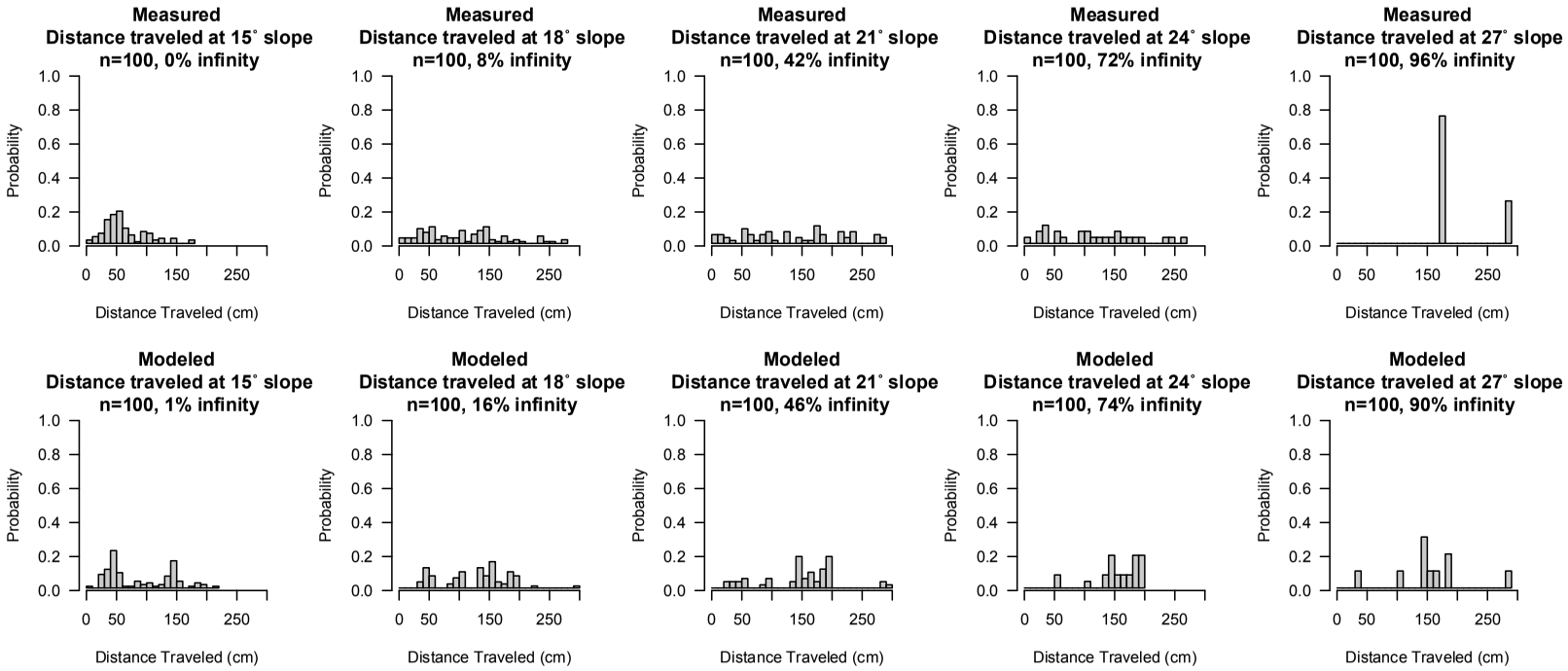

Figure 5 (continued).

$$f(x \mid p) = \begin{cases} p, & x = 1, \\ 1 - p, & x = 0, \\ 0, & \text{otherwise}, \end{cases} \tag{2}$$

where p is a function of flume angle, θ, given by the logistic equation:

$$p(\theta) = \frac{e^{\beta_0 + \beta_1 \theta}}{1 + e^{\beta_0 + \beta_1 \theta}}, \tag{3}$$

where β_0 and β_1 were obtained by performing a logistic regression on the flume data (Table 1).

Let Y be a random variable that represents the distance traveled by a particle on the flume, given that it did not fall off the end. If the outcome of the above Bernoulli trial is a success, Y $\sim$ Beta$(\alpha, \beta, 0, L)$. If the outcome of the above Bernoulli trial is a failure, the distance traveled is "infinity." The conditional density function of Y is given by:

$$f(y \mid x) = \begin{cases} \text{Beta}(\alpha, \beta, 0, L), & x = 1, \\ \text{“infinity,”} & x = 0, \\ 0, & \text{otherwise}, \end{cases} \tag{4}$$

where the probability density function for Beta$(\alpha, \beta, 0, L)$ is given by:

$$f(y \mid \alpha, \beta, 0, L) = \begin{cases} \left[\dfrac{1}{L} \cdot \dfrac{\Gamma(\alpha + \beta)}{\Gamma(\alpha) \cdot \Gamma(\beta)} \right] \left(\dfrac{y}{L}\right)^{\alpha - 1} \left(1 - \dfrac{y}{L}\right)^{\beta - 1}, & 0 < y < L, \\ 0, & \text{otherwise}, \end{cases} \tag{5}$$

where L is the length of the flume and α and β are each nonlinear functions of

Table 1. Regression Coefficients.

β_0	13.511	a_1	1.0E-04	b_1	-4.0E-04
β_1	-0.614	a_2	-0.005	b_2	0.028
		a_3	0.051	b_3	-0.660
		a_4	-0.002	b_4	4.526
		a_5	1.428	b_5	13.193

Regression coefficients, β_n, for logarithmic regression on p and θ ($r^2 = 0.836$); a_n, for polynomial regression on α and θ ($r^2 = 0.908$); b_n, for polynomial regression on β and θ ($r^2 = 0.979$).

flume angle, θ, of the form:

$$\alpha(\theta) = a_1\theta^4 + a_2\theta^3 + a_3\theta^2 + a_4\theta + a_5, \tag{6}$$

$$\beta(\theta) = b_1\theta^4 + b_2\theta^3 + b_3\theta^2 + b_4\theta + b_5, \tag{7}$$

where a_n and b_n are the coefficients of polynomial regression (Table 1). Beta distributions were fit to the results at each flume angle setting via maximum likelihood estimation, from which an estimate of α and β were obtained for each flume angle (Table 2; Fig. 6). These were then plotted against flume angle and 4^{th} order polynomial regressions were performed to obtain estimates of the constants in equations 6 and 7.

DISCUSSION

Model

The motion of particles down a rough surface can be characterized by the equation for a body sliding down an inclined plane:

$$x = \frac{v_o^2}{2g(\mu cos\theta - sin\theta)}, \tag{8}$$

where x is the distance traveled and μ is the coefficient of kinetic friction (Gabet, 2003). If the roughness of the flume surface were uniform, a single value of μ could be used to calculate transport distances according to equation 8. However, because the surface was irregular, a spatial distribution of roughness values was needed to model transport distances. Equation 8 can be rearranged to yield:

Table 2. Shape Parameters for Fitted Distributions.

	Fitted α	Fitted β	Measured Mean	Fitted Mean	Measured Stdv	Fitted Stdv
0°	1.315	12.593	28.47	28.37	22.14	22.73
3°	1.962	23.346	23.33	23.26	14.66	15.64
6°	2.565	21.210	32.44	32.36	17.95	18.70
9°	2.182	16.844	34.61	34.41	19.40	21.36
12°	2.514	13.196	48.01	48.01	27.17	26.91
15°	2.594	9.742	62.70	63.09	35.18	33.48
18°	1.339	2.358	107.42	108.66	67.50	66.53
21°	1.036	1.292	135.12	133.48	83.43	81.72
24°	1.283	2.011	116.81	116.85	73.37	70.60
27°	4.054	1.816	203.38	207.17	53.09	52.91

Shape parameters α and β for beta distributions fit to experimental results via maximum likelihood estimation.

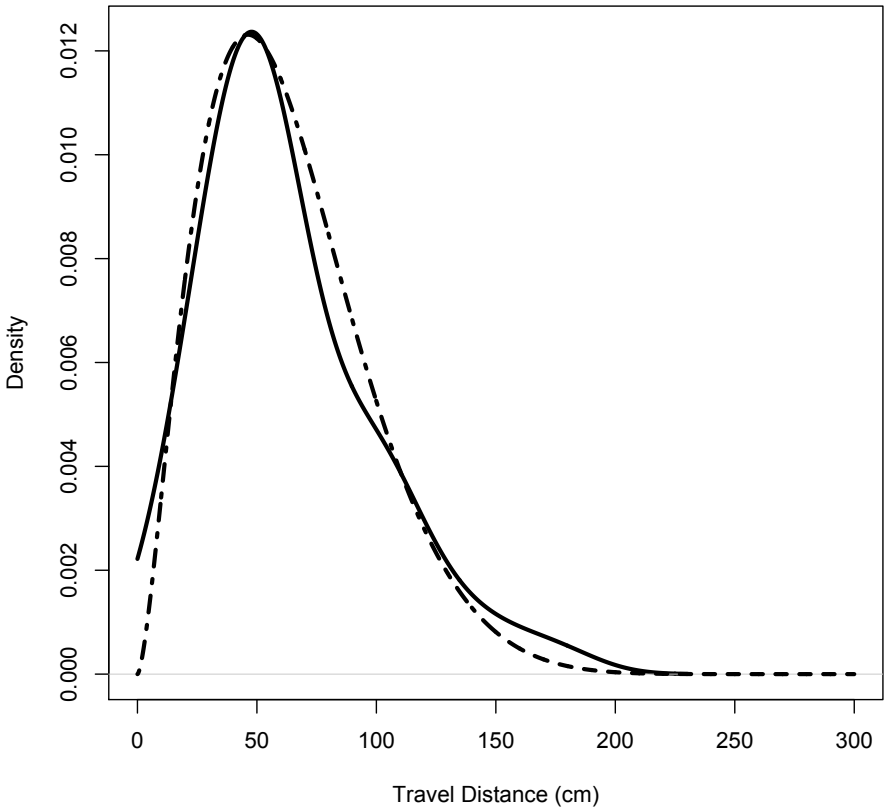

Figure 6. Example of a beta distribution fit to experimental results. The solid line represents the empirical density function for flume results at 15° and the dashed line represents the density function of the beta distribution fitted to 15° via maximum likelihood estimation.

$$\bar{\mu} = \frac{v_o^2}{2gxcos\theta} + tan\theta, \tag{9}$$

where $\bar{\mu}$, a friction coefficient spatially averaged over the distance x, can be calculated from each measured transport distance to create a distribution of $\bar{\mu}$ values.

The 812 measurements of the flume relief characterize the roughness of the surface in the experiments; however, these values are not necessarily transferable to other situations. To create a general approach that can be used in future studies, and to make the measured roughness of the flume unitless (and thus dimensionally equivalent to a coefficient of friction), the values of surface roughness of the flume were divided by the diameter of the transported pebbles (1 cm) to create a distribution of relative roughness values. Because both the relative roughness values and the $\bar{\mu}$ values from the 0°-angle experiments follow exponential distributions (Fig. 7), the distribution of the former could be mapped onto the latter. The transport distances from the experiments at 0° were used because, at this low angle, the pebbles bounced the least and therefore spent the most time in contact with the floor of the flume, making it the best distribution to characterize the flume surface. Converting the relative roughness values to μ values was accomplished by transforming the mean value of the relative roughness distribution into that of the coefficient of kinetic friction distribution by multiplying by the ratio of the mean of the coefficients of kinetic friction at 0° and the mean of the relative roughness values. The minimum of the coefficient of kinetic friction values was then added to the result. The result of this transformation is a distribution of μ values that characterizes the roughness of the flume and that can be used in a numerical model to simulate particle transport down a rough surface.

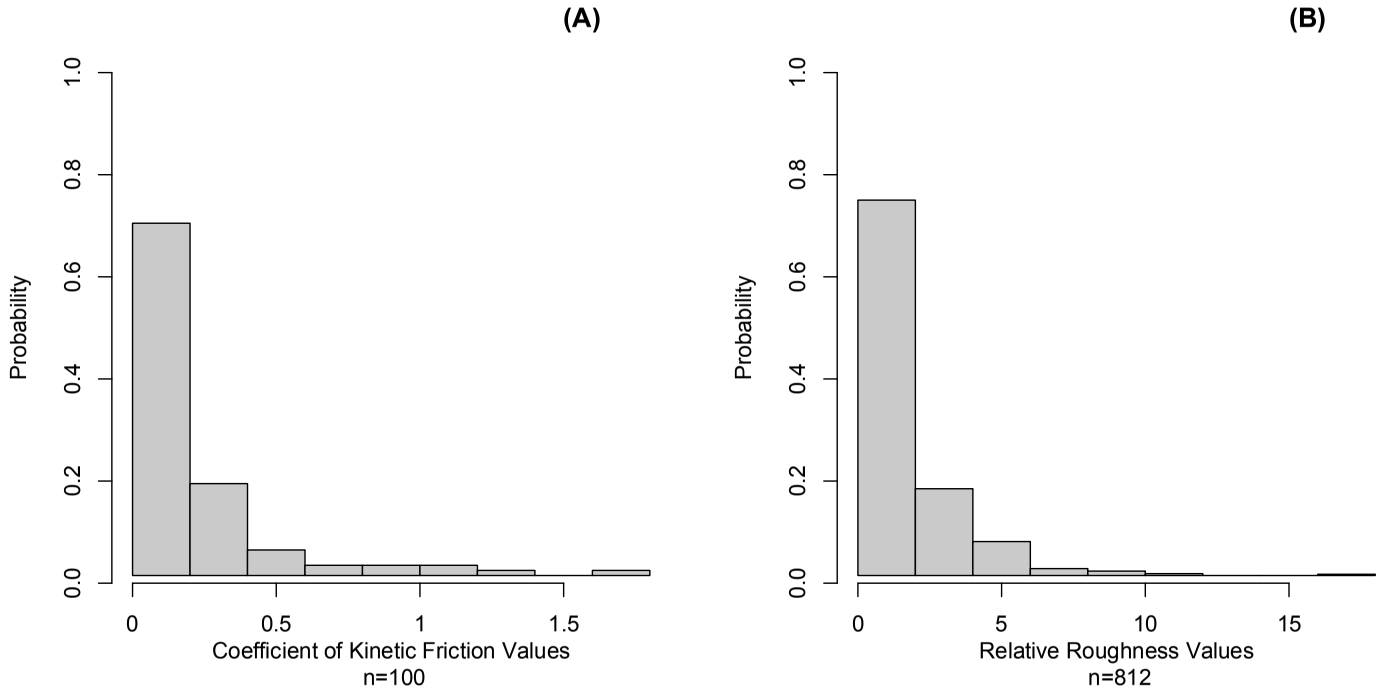

Figure 7. (A) Distribution of μ values calculated from results of flume experiment at 0°. (B) Distribution of relative roughness values measured from flume surface.

A computer model was developed (see Appendix I) to approximate the physics of a particle sliding and bouncing down a rough surface. If the experimental results are reproduced, then this method can be used to model the evolution of entire hillslopes. The model simulates a particle with an initial velocity of 0.7 m/s traveling down a rough surface that is 3-m-long. The distance traveled, x, is calculated according to:

$$x = v\Delta t, \tag{10}$$

where v is velocity and Δt is the time step (s). The length of the time step was adjusted down until the model fit the experimental results. The velocity is updated at each time step according to:

$$v = c(v_o + a\Delta t), \tag{11}$$

where c is a coefficient of restitution, with values between 0 and 1, that accounts for energy lost during collisions of the particle with the surface. The acceleration, a, is calculated with:

$$a = g(sin\theta - \mu cos\theta). \tag{12}$$

At each time step, a value for μ is randomly chosen from the probability distribution derived earlier (Fig. 7) based on its location. The particle is advanced, according to equations 10-12, until its velocity is calculated to be a non-positive number or its total transport distance exceeds 3 m (Fig. 8).

Comparisons

Model results are compared to the results from the flume experiments in

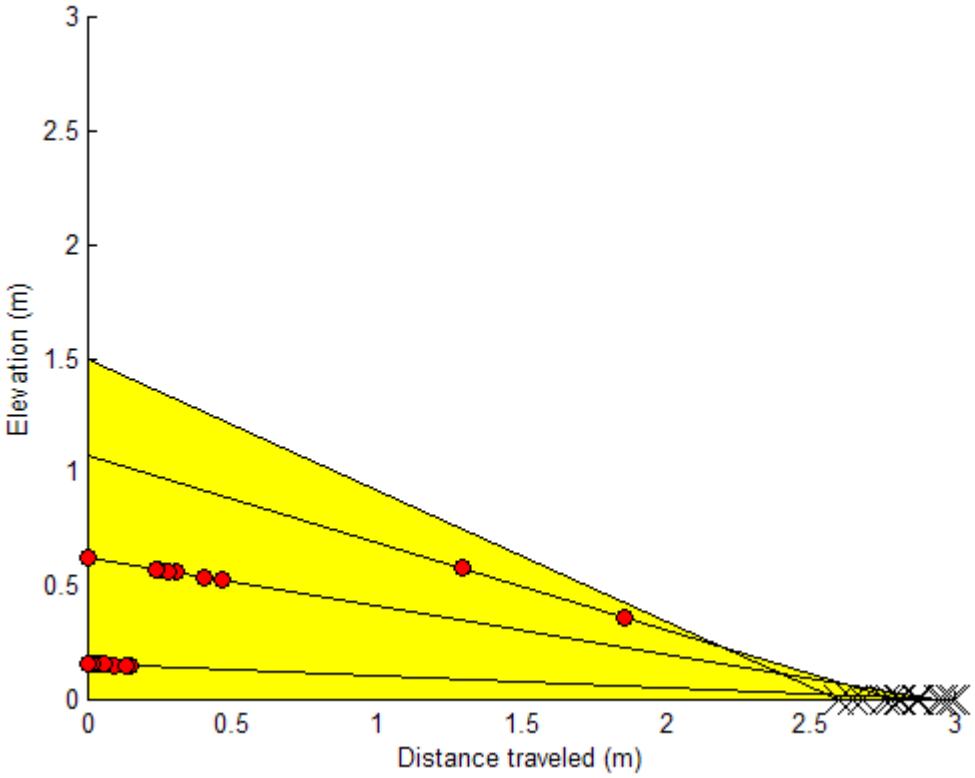

Figure 8. Example run of model output for 3°, 12°, 21°, and 30° slopes. Diagonal lines represent modeled flume surface. Shaded circles represent particles that have stopped on the modeled flume surface and X's represent particles that reached the end.

Table 3 and Figure 5. At a significance level of $\alpha = 0.05$, there was a difference between 6 of the means of measured transport distances and their corresponding means of modeled transport distances. The difference in mean transport distances ranged from 18% to 63% at the slopes of 0°, 3°, 6°, 15°, 18°, and 24°. At a significance level of $\alpha = 0.05$, none of the differences in sample proportions of the number of particles that rolled to the end of the flume are significant.

The model is scale-independent. It currently runs for a particle size of 1 cm, but by scaling the distribution of coefficients of kinetic friction values by the appropriate factor, smaller or larger particles could be modeled. A smaller particle would experience more resistance from the flume surface and would therefore travel shorter distances, on average. A larger particle would experience less resistance from the flume surface and would therefore travel farther, on average.

Currently the model selects from a roughly exponential distribution of coefficient of kinetic friction values (Fig. 7), thus, on average, smaller values of μ are chosen over larger ones. If a small value for the coefficient of kinetic friction is selected, the particle will travel farther compared to when a larger value for the coefficient of kinetic friction is chosen. If the model were instead selecting from a different distribution of coefficient of kinetic friction values, the results would likely be different. For example, if the model were selecting from a normal distribution, larger values of μ would be selected more often, and thus, on the average, the particles would not travel as far.

The results of the experiments of Roering (2004) suggested that the travel distance of particles near the surface is best characterized probabilistically, which was the case in this study (Fig. 5). Given the probabilistic nature of travel distances of particles on an inclined surface, one would not expect the modeled results to match the experimental results perfectly. Nevertheless, the model is able

Table 3. Comparison of Experimental and Modeled Results.

Flume angle (°)		Sample mean ± s.e. (cm)	P-value from Mann-Whitney *U* test †	Proportion rolled to end ± s.e. (%)	P-value from Fisher's exact test †
0	Measured	28.5 ± 2.2	2.36e-09 *	0	1
	Modeled	10.7 ± 0.6		0	
3	Measured	23.3 ± 1.5	1.75 e-04 *	0	1
	Modeled	15.4 ± 0.7		0	
6	Measured	32.4 ± 1.8	1.39 e-03 *	0	1
	Modeled	24.0 ± 0.7		0	
9	Measured	34.6 ± 1.9	0.589	0	1
	Modeled	32.4 ± 1.4		0	
12	Measured	48.0 ± 2.7	0.755	0	1
	Modeled	48.5 ± 3.1		0	
15	Measured	62.7 ± 3.5	0.0155 *	0	1
	Modeled	87.1 ± 5.4		1 ± 1	
18	Measured	107.4 ± 7.0	0.0125 *	8 ± 3	0.126
	Modeled	126.2 ± 6.0		16 ± 4	
21	Measured	135.1 ± 11.0	0.371	42 ± 5	0.669
	Modeled	149.2 ± 8.5		46 ± 5	
24	Measured	116.8 ± 13.9	0.0116*	72 ± 5	0.874
	Modeled	159.0 ± 7.6		74 ± 4	
27	Measured	203.4 ± 26.5	0.179	96 ± 2	0.164
	Modeled	155.0 ± 19.9		90 ± 3	
30	Measured	N/A §		100	0.246
	Modeled	163.7 ± 15.6		97 ± 2	

Summary table of measured and modeled transport distances for 0 through 30 degrees. Average distances traveled at each slope are given along with their standard deviation. The p-values from the Mann-Whitney U test for detecting a location shift are reported for each slope. The sample proportions of particles that rolled to the end of the flume, or past 3 m in the case of the model, are given along with their standard deviations. P-values are also reported for Fisher's exact test for difference in population proportions.

* There is a difference in sample means at significance level $\alpha = 0.05$.

§ All 100 pebbles rolled to the end of the flume.

† See Appendix II for details.

to reproduce the general shapes of the distributions of transport distances (Fig. 5), some of the means perfectly (Table 3), and others with a percent difference that ranges from 18-63%. The model is also able to reproduce the proportion of pebbles that roll to the end of the flume perfectly (Table 3). Thus, the model is able to reproduce the experimental results reasonably well, and it fulfills the other goals of the study in that it (1) depends on roughness and slope, (2) is based on the essential physics of the problem, and (3) is parsimonious.

The results of the experiments show that the transport distances of particles due to dry ravel do not have an exponential distribution (Fig. 5), as was used in the model of Furbish and Haff (2010) as a general starting point for all types of particle transport on hillslopes. The data confirm the hypothesis of Furbish and Haff (2010) that different transport processes and environments exhibit different types of characteristic distributions that depend on both gradient and surface roughness. Furbish and Haff (2010) proposed that sediment characteristics were also likely to be involved. The current model takes the size of the particles into account by scaling the roughness values according to the particle size, which were subsequently trasformed into μ values, but the kinematic equations 10-12 used to model the motion of particles in this experiment are independent of particle mass and shape. A promising starting point for future study would be to incorporate additional parameters for particle characteristics, such as sphericity and roundness, into the model that was developed for this study.

CONCLUSIONS

Experiments were performed in which the travel distance of pebbles released into a dry ravel flume was measured. The results were used to create probability

distributions that characterize the travel distance of particles down a rough surface. A numerical model for particles traveling down a rough surface was then created, and the results produced by the model were compared with the results of the flume experiments. Since the model was able to successfully reproduce the experimental results, it has the potential to be used with inputs measured from the field to model the evolution of entire hillslopes. The sediment flux produced by the model could be calculated and the parameters adjusted to bring the sediment flux rate into agreement with rates observed in nature in an attempt to produce hillslopes with planar mid-slope sections.

REFERENCES CITED

Anderson, R. S., 1994, Evolution of the Santa Cruz Mountains, California, through tectonic growth and geomorphic decay: Journal of Geophysical Research, v. 99, p. 20161-20179.

Culling, W. E. H., 1960, Analytical theory of erosion: Journal of Geology, v. 68, p. 336-344.

Culling, W.E.H, 1963, Soil creep and the development of hillside slopes: Journal of Geology, v. 73, p. 127-161.

Fisher, R. A., 1922, On the interpretation of χ^2 from contingency tables, and the calculation of p: Journal of the Royal Statistical Society, v. 85, p. 87-94.

Furbish, D. J., Hamner, K. K., Schmeeckle, M. N., Borosund, M. N., Mudd, S. M., 2007, Rain splash of dry sand revealed by high-speed imaging and sticky-paper splash targets: Journal of Geophysical Research, v. 112, F01001, doi: 10.1029/2006JF000498.

Furbish, Childs, E., M., Haff, P. K., and Schmeeckle, M. W., 2009, Rain splash of soil grains as a stochastic advection-dispersion process, with implications for desert plant-soil interactions and land-surface evolution: Journal of Geophysical Research, v. 114, F00A03, doi: 10.1029/2009JF001265.

Furbish, D. J., and Haff, P. K., 2010, From divots to swales: Hillslope sediment transport across divers length scales: Journal of Geophysical Research, doi:10.1029/2009JF001276 (in press).

Gabet, E. J., 2000, Gopher bioturbation: Field evidence for non-linear hillslope diffusion: Earth Surface Processes and Landforms, v. 25, p. 1419-1428.

Gabet, E. J., 2003, Sediment transport by dry ravel: Journal of Geophysical Research, v. 108, doi: 10.1029/2001 JB001686.

Kirkby, M. J., 1985, A model for the evolution of regolith-mantled slopes, *in* Woldenberg, M. J., ed., Models in geomorphology: London, Allen & Unwin, p. 213-238.

Roering, J. J., Kirchner, J. W., and Dietrich, W. E., 1999, Evidence for non-linear, diffusive sediment transport on hillslopes and implication for landscape morphology: Water Resources Research, v. 35, p. 853-870.

Roering, J. J., Kirchner, J. W., Sklar, L. S., and Dietrich, W. E., 2001, Hillslope evolution by nonlinear creep and landsliding: An experimental study: Geology, v. 29, p. 143-146.

Roering, J. J, 2004, Soil creep and convex-upward velocity profiles: Theoretical and experimental investigation of disturbance-driven sediment transport on hillslopes: Earth Surface Processes Landforms, v. 29, p. 1597-1612.

Schumer, R., Meerschaert, M. M., and Baeumer, B., 2009, Fractional advection-dispersion equations for modeling transport at the Earth surface: Journal of Geophysical Research, v. 114, doi: 10.1029/2008JF001246.

Tucker, G.E., and Bradley, D.N., 2010, Trouble with diffusion: Reassessing hillslope erosion laws with a particle-based model: Journal of Geophysical Research, v. 115, doi: 10.1029/2009JF00126.

Wackerly, D. D., Mendenhall, W., Scheaffer, R. L., 2008, Mathematical Statistics with Applications, 7^{th} ed.: Belmont, California, earBrooks/Cole.

APPENDIX I: MATLAB CODE

```
% Discrete element model for tracking one particle
% Created by Morgan Mendoza
% Last modified June 2, 2010

clear all
close all

% Assign constants
        TS = 0.1;      % Time step (sec)
        g = 9.81;      % Acceleration due to gravity (m/s^2)
        length = 3;    % Length of the ramp (m)

% Initialize vectors and matrices
        results = zeros(100,11);                          % Results storage
        sin_theta_previous = zeros(max_angle_index,1);    % Used for graphics
        cos_theta_previous = zeros(max_angle_index,1);    % Used for graphics
        max_angle_index = 10;

% Load matrix with mu values and calculate dimensions
        load -ascii roughness_new_0.txt
        mymodelmunew = roughness_new_0;
        [nrow,ncol] = size(mymodelmunew);

% ******************MAIN LOOP*******************

for angle_index = 0 : max_angle_index

        % Ramp angle in increments of 3 degrees
        theta = 3 * angle_index;

        % Convert to radians, used in calculations
        sin_theta = sin(theta * pi/180);
        cos_theta = cos(theta * pi/180);

        % Used for graphics
        sin_theta_previous(angle_index+1, 1) = sin_theta;
        cos_theta_previous(angle_index+1, 1) = cos_theta;

        % Initialize the figure
```

```
% Plot the ramp
figure(1);
xlabel('X (m)');
ylabel('Elevation (m)');
x_patch = [0 length * cos_theta 0];
y_patch = [length * sin_theta 0 0];
f = patch(x_patch, y_patch, 'b');
axis([0 3 0 2.5]);

% Keep lines from old slope setting present on current slope setting
for next_slope = 1 : angle_index
    x_patch = [0 length * cos_theta_previous(next_slope)];
    y_patch = [length * sin_theta_previous(next_slope) 0];
    h = patch(x_patch, y_patch,'b');
end

hold on

% 100 pebble runs
for run_index = 1:100

    old_velocity = 0.7;
    x_position = 0;                    % This is where the rock starts
    z_position = length * sin_theta;   % This is the top of the ramp
    ramp_position = 0;                 % Start at top of ramp
    p = plot(x_position, length * sin_theta, 'o', 'markeredgecolor', 'k', ...
        'markerfacecolor', 'r', 'erasemode', 'xor');
    pause(.05)
    x = 1; % Initially mu is selected from the values at the top of the ramp

    % Keep going while the rock is still moving
    while old_velocity > 0

        % Select mu for new time step
        if x <= 0
            x = 1;
        end

        temp = ceil(nrow * rand); % Randomly selects an index value
        mu = mymodelmunew(temp, x);

        % Calculate velocity and distance travelled
```

```
        new_velocity = g * TS * (sin_theta - mu * cos_theta) + old_velocity;
        if new_velocity < 0
                new_velocity = 0;
                break
        end

        distance = new_velocity * TS;

        % Calculate x and z components of distance
        x_distance = cos_theta * distance;
        z_distance = sin_theta * distance;

        % Add distance travelled in this time interval to present location
        x_position = x_position + x_distance;
        z_position = z_position - z_distance;

        % Keep track of distance traveled and select from appropriate mu
        ramp_position = ramp_position + distance;
        x = ceil(ramp_position/.10);
        if x >= 29
                x = ceil(rand * 28);
        end

        % Change the slope and z_position when the rock leaves the ramp
        if ramp_position > length
                ramp_position = -1; % Infinity indicator
                new_velocity = 0;
                set(p, 'Xdata', min(300, x_position), 'Ydata', 0);
                set(p, 'Marker', 'x','MarkerSize', 15, 'markerfacecolor', 'g',...
                        'markeredgecolor', 'k');
                pause(.05)
        else % Plot the position of the rock
                set(p, 'Xdata', x_position, 'Ydata', z_position);
                pause(0.1)
        end

        % Assign starting velocity for next time step
        old_velocity = c * new_velocity;

end % End while old_velocity > 0

% Record results
```

```
            results(run_index, angle_index+1) = ramp_position;

        end % End run_index

end % End angle_index
```

APPENDIX II: STATISTICAL NOTES

The statistical computing program, R, was used for all statistical calculations. Wackerly et al. (2008) was used for interpretations and explanations of p-values and the Mann-Whitney U test, and Fisher (1922) was used for Fisher's exact test.

Interpreting P-Values

P-values are the probability of observing an event similar to what was observed, or more extreme, given that the null hypothesis is true. In the case of comparing the sample means of the distance traveled, the p-value represents the probability of observing a difference in the sample means as great as or greater than what was observed, given that the samples were taken from an identical population. In the case of comparing the sample proportions, the p-value represents the probability of observing a difference in the sample proportions as great as or greater than what was observed, given that the two samples are coming from the same population. A small p-value would indicate that it is unlikely that the two samples are coming from the same population. In the instances where the difference in the sample proportions are zero, the p-values are 1 because there is nothing less extreme than seeing no difference in the sample proportions, and thus, the probability of seeing a difference as great as was observed, or greater, would have to be 1.

Mann-Whitney U Test

The Mann-Whitney U test is a non-parametric test that can be performed

when there is reason to believe that the data in question are not normally distributed. Both the Z-test and t-test require that normality assumptions be made. However, if these assumptions are violated, then the resultant p-value will not be accurate. The data from the flume experiments are not normally distributed (Fig. 5) and thus neither a Z-test, nor a t-test can be used to test for a difference in population means. The Mann-Whitney U test is commonly applied when there is doubt surrounding the validity of assuming normality because it does not require that any normality assumptions be made, only that the data are independent and identically distributed. The null hypothesis is that the data are coming from the same distribution with no location shift. No assumptions are made about the type or shape of the distribution. The alternative hypothesis is that the data are coming from the same distribution, but that the distributions are shifted in location. Even in cases where a Z-test or t-test is valid, the efficiency of the Mann-Whitney U test is almost as good as the Z-test and t-test. The efficiency of the Mann-Whitney U test may be much higher in cases where the Z-test or t-test cannot be performed.

Fisher's Exact Test

Fisher's exact test uses exact binomial probabilities to test whether two populations have the same probability of an event occurring. The null hypothesis is that the odds ratio is 1, implying that the chance of observing an event in population 1 is the same as in population 2. Fisher's exact test was used rather than the simpler Z-test or Pearson's χ^2 test because neither test would have been valid in this instance. The Z-test is not valid when n_1p_1, $n_1(1-p_1)$, n_2p_2, or $n_2(1-p_2)$ is less than 5, where n_1 and n_2 are the sizes of samples 1 and 2 and p_1 and p_2 are the probability of success in populations 1 and 2. These calculations are

less than 5 in the instances where the observed sample proportions are close to zero or one. Pearson's χ^2 test breaks down when any of the expected cell counts in a 2x2 contingency table are less than 5, which occurs when the sample proportions are close to 0 or 1. Fisher's exact test avoids these issues by calculating exact binomial probabilities and can be used regardless of sample characteristics. Fisher's exact test is more computationally intensive than either the Z-test or Pearson's χ^2 test, but with modern computers, Fisher's exact test can be performed quickly. Fisher's exact test does require fixed margins, which are not achieved in this case and indeed are rarely achieved in practice. However the fact that the margins are not fixed mainly affects the calculations of the power of the test and not the p-value. Therefore, even though all of the assumptions of Fisher's exact test are not met, it can still be used and its resultant p-value can be trusted.